Asian Journal of Control, Vol. 21, No. 1, pp. 354–363, January 2019
Published online 24 October 2018 in Wiley Online Library (wileyonlinelibrary.com) DOI: 10.1002/asjc.1916

STATE ESTIMATION FOR AN AGONISTIC-ANTAGONISTIC MUSCLE SYSTEM

Thang Tien Nguyen, Holly Warner, Hung La, Hanieh Mohammadi, Dan Simon and Hanz Richter

ABSTRACT

Research on assistive technology, rehabilitation, and prosthetics requires the understanding of human machine interaction, in which human muscular properties play a pivotal role. This paper studies a nonlinear agonistic-antagonistic muscle system based on the Hill muscle model. To investigate the characteristics of the muscle model, the problem of estimating the state variables and activation signals of the dual muscle system is considered. In this work, parameter uncertainty and unknown inputs are taken into account for the estimation problem. Three observers are presented: a high gain observer, a sliding mode observer, and an adaptive sliding mode observer. Theoretical analysis shows the convergence of the three observers. Numerical simulations reveal that the three observers are comparable and provide reliable estimates.

Key Words: Adaptive sliding mode, high gain observer, Hill muscle model, human muscles, state estimation, sliding mode observer.

I. INTRODUCTION

The design of prosthetic, orthotic, and functional neuromuscular stimulation systems requires the understanding of the coordination of the human body and the dynamical properties of muscles [1]. The intermuscular coordination can be studied based on classical models proposed by Hill, Wilkie, and Richie [1]. The most widely implemented model for simulating human muscles is the Hill model [2].

Human muscles operate at many joints. For a given joint, muscles often act in pairs with one or more muscles on opposite sides. Each member of a pair is regarded as an agonist or antagonist. In this paper, an agonistic-antagonistic muscle system based on the Hill muscle model is introduced to study coordination and estimate muscle parameters.

A variety of estimation problems for different muscle models have been addressed. In [3], muscle forces, joint moments, and/or joint kinematics are estimated from electromyogram signals using forward dynamics. In [4], the estimation problem of individual muscle forces during human movement is solved using forward dynamics. In [5], the muscular torque is estimated using a nonlinear observer in a sliding mode controller of a human-driven knee joint orthosis. In [6], the estimation of muscle activity is conducted using higher-order derivatives, static optimization, and forward-inverse dynamics. In [7], an inverse dynamic optimization problem is proposed to estimate muscle and contact forces in the knee during gait.

There have been numerous estimation methods proposed to observe nonlinear systems, from high gain observers to sliding mode observers; see [8–11] and references therein. High gain observers can offer a high level of accuracy in estimating state variables and uncertainties [10,11]. Sliding mode observers exhibit similar performance in estimating state variables and unknown inputs [8,9,12,19–22]. A recent work [20] studies sliding mode control in combination with fuzzy logic to deal with matched/unmatched uncertainties and external disturbances. In [19], sliding mode based estimation control schemes are presented to deal with actuator faults and system uncertainties for robotic systems. Therefore, sliding mode observers, which are based on sliding mode control, can be employed to address many problems in fault detection and isolation, in which important param-

Manuscript received February 26, 2018; revised June 10, 2018; accepted June 26, 2018.

Thang Tien Nguyen (corresponding author, e-mail: nguyentienthang@tdtu.edu.vn) is with Modeling Evolutionary Algorithms Simulation and Artificial Intelligence, Faculty of Electrical & Electronics Engineering, Ton Duc Thang University, Ho Chi Minh City, Vietnam.

Holly Warner and Hanz Richter are with the Department of Mechanical Engineering, Cleveland State University, Cleveland, OH 44115, USA.

Hung La is with the Advanced Robotics and Automation (ARA) Lab, Department of Computer Science and Engineering, University of Nevada, Reno, NV 89557, USA.

Hanieh Mohammadi and Dan Simon are with the Department of Electrical Engineering and Computer Science, Cleveland State University, Cleveland, OH 44115, USA.

This work was supported by National Science Foundation grant 1544702.

eters such as state variables, faults or unknown inputs need to be reconstructed from the available information. While traditional sliding mode techniques require the knowledge of unknown inputs and uncertainties, recent adaptive sliding mode control methods have been developed to overcome this limit at the cost of complexity [13,14].

In this paper, we aim to design a high gain observer, a conventional sliding mode observer, and a new adaptive sliding mode observer for our dual muscle system.

The contribution of our research work lies in the construction and development of a high gain observer, a sliding mode observer, and an adaptive sliding mode observer for the agonistic-antagonistic muscle system where unknown inputs are taken into account. The high gain observer is designed based on recent results in [10,11], which allows estimation of state variables and unknown inputs, from which activation signals are constructed. The conventional sliding mode observer is built based on the first order sliding mode and super-twisting algorithm developed in [9,15], for which bounds of unknown control inputs and uncertainty need to be known. The third observer is developed based on recent results on dual layer adaptive sliding mode control [13,14], which does not require knowledge of the bounds of unknown inputs and uncertainty.

It is noted that the estimation problem of the nonlinear agonistic-antagonistic muscle system with unknown inputs and uncertainties has not been fully addressed. Hence, the novelty of the paper is the exploitation of recent developments of estimation based on high-gain and sliding mode approaches for the dual muscle system based on the Hill muscle model. The theoretical convergence proofs are provided to show the applicablity of the observers to the dual muscle system with unknown inputs and uncertainties.

II. PROBLEM FORMULATION

We study the agonistic-antagonistic muscle system where each muscle is based on the Hill muscle model [1]. The Hill muscle unit models several effects of the physical muscle. It is divided into two sections: the tendon and the muscle body. The tendon is modeled as a nonlinear stiffness that includes some amount of slack. Within the muscle body portion of the model, a nonlinear stiffness element, modeled similarly to the tendon, and a force generation element are oriented in parallel. The tendon and muscle body components are then placed in series. The structure of the dual muscle system is described in Fig. 1, where the abbreviations *CE*, *SEE*, and *PE* stand for the contractile, series elastic, and parallel elastic elements of the Hill muscle model. Because muscles can only apply force when contracting, two muscles are required to actuate the central mass m, which is a simple load selected for studying the fundamental dynamics of this system.

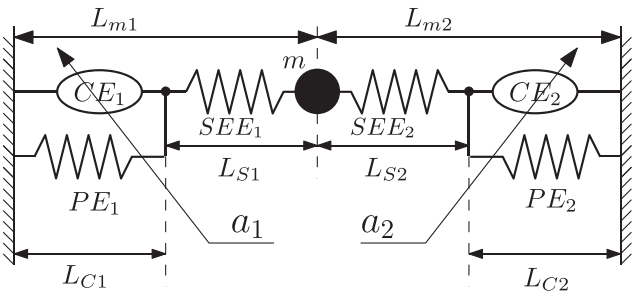

Fig. 1. Two-muscle, one degree-of-freedom agonistic-antagonistic system with mass load [16].

The lengths of the *CE* and *SEE* are denoted as L_{Cj} and L_{Sj} for muscle j ($j = 1, 2$), and the total length of the jth muscle is defined by

$$L_{mj} = L_{Cj} + L_{Sj}. \tag{1}$$

Let L_{m1} be the position of the mass in Fig. 1, and the corresponding velocity is positive to the right.

The dual muscle system possesses the following dynamics [16,17]

$$\dot{x}_1 = x_2 \tag{2}$$

$$\dot{x}_2 = \frac{1}{m}(\Phi_{S2}(L_{S2}) - \Phi_{S1}(L_{S1})) + \Delta_\Phi(\tau) \tag{3}$$

$$\dot{L}_{S1} = x_2 + g_1^{-1}(z_1) \tag{4}$$

$$\dot{L}_{S2} = -x_2 + g_2^{-1}(z_2) \tag{5}$$

where

$$x_1 \triangleq L_{m1}, \tag{6}$$

$$z_j = \frac{\Phi_{Sj}(L_{Sj}) - \Phi_{Pj}(L_{Cj})}{a_j f_j(L_{Cj})} \text{ for } j = 1, 2, \tag{7}$$

where Φ_{Sj} is the elastic force, Φ_{Pj} is the parallel elastic force, a_j is the activation signal of element j with $a_j \in [0, 1]$, and $\Delta_\Phi(\tau)$ is a bounded uncertainty. The force-length dependence factor f_j has the general shape of a Gaussian curve, and the velocity dependence function $g_j^{-1}(z_j)$ obeys the Hill model:

$$f_j(L_{Cj}) = \exp\left[-\left(\frac{L_{Cj} - 1}{W}\right)^2\right] \tag{8}$$

$$g_j^{-1}(z_j) = \begin{cases} \frac{1-z_j}{1+z_j/A}, & z_j \le 1 \\ \frac{-A(z_j-1)(g_{max}-1)}{(A+1)(g_{max}-z_j)}, & z_j > 1 \end{cases} \quad (9)$$

where W, A, and g_{max} are positive parameters. Denote

$$u_1 \triangleq g_1^{-1}(z_1) \quad (10)$$

$$u_2 \triangleq g_2^{-1}(z_2) \quad (11)$$

as the virtual control inputs of the system (2), (3), (4), (5).

We have the following assumptions for our system.

Assumption 1. The uncertainty $\Delta_\Phi(\tau)$ satisfies

$$|\Delta_\Phi(\tau)| < \Delta_m \quad (12)$$

where Δ_m is a positive constant.

Remark 1. $\Delta_\Phi(\tau)$ can represent parameter uncertainties due to model mismatch; for example, uncertainties in the description of $\Phi_{Sj}(L_{Sj})$ and the mass m.

Assumption 2. The control inputs of the system (2), (3), (4), (5) satisfy

$$|u_j(\tau)| < U_{jm} \text{ for } j = 1, 2 \quad (13)$$

where U_{jm} is a positive constant.

The length constraint of the dual muscle system is

$$L_{m1} + L_{m2} = C \quad (14)$$

where C is a constant. Hence, L_{C1} and L_{C2} will be determined from the relations in (1) and (14) if C, L_{S1}, L_{S2}, and L_{m1} are available. Therefore, it is sufficient to consider four differential equations of the model in (2), (3), (4), and (5) for our estimation problem. From (1), (4), (5), and (14), the dynamics of L_{C1} and L_{C2} are described as

$$\dot{L}_{C1} = -g_1^{-1}(z_1) \quad (15)$$

$$\dot{L}_{C2} = -g_2^{-1}(z_2). \quad (16)$$

The nonlinear functions Φ_{Sj}, Φ_{Pj}, f_j, and g_j^{-1} ($j = 1, 2$) can be found in [16,17]. All the variables and functions of the dual muscle system are normalized to simplify the dynamics.

Assume that x_1, $\Phi_{S1}(L_{S1})$, and $\Phi_{S2}(L_{S2})$ are available. The mass position can be tracked by a sensor while the *SEE* nonlinear spring forces $\Phi_{S1}(L_{S1})$ and $\Phi_{S2}(L_{S2})$ of the agonistic-antagonistic muscles can be measured by two load cells, from which L_{Sj} is inferred due to the inverse of $\Phi_{Sj}(L_{Sj})$. The observability matrix of the dual muscle system can be calculated using the Lie derivatives of the outputs, and it has rank 4, implying that the dual muscle system is locally observable [18].

For ease of presentation, let

$$x_3 \triangleq L_{S1} \quad (17)$$

$$x_4 \triangleq L_{S2}. \quad (18)$$

Due to the relations (1) and (14), L_{Cj} can be deduced from L_{mj} and L_{Sj}. Our system is rewritten as

$$\dot{x}_1 = x_2 \quad (19)$$

$$\dot{x}_2 = \frac{1}{m}(\Phi_{S2}(x_4) - \Phi_{S1}(x_3)) + \Delta_\Phi(\tau) \quad (20)$$

$$\dot{x}_3 = x_2 + u_1(x) \quad (21)$$

$$\dot{x}_4 = -x_2 + u_2(x) \quad (22)$$

$$y_1 = x_1 \quad (23)$$

$$y_2 = \Phi_{S1}(x_3) \quad (24)$$

$$y_3 = \Phi_{S2}(x_4) \quad (25)$$

where $x = \begin{bmatrix} x_1 & x_2 & x_3 & x_4 \end{bmatrix}^T$, and the vector $y = \begin{bmatrix} y_1 & y_2 & y_3 \end{bmatrix}^T$ is the output of the dual muscle system. Note that from the measurement of y_2 and y_3, x_3 and x_4 can be calculated due to the inverse of the function $\Phi_{Sj}(L_{Sj})$. Let

$$u = \begin{bmatrix} u_1 & u_2 \end{bmatrix}^T. \quad (26)$$

Given the measurements of the length of the agonistic muscle and muscle forces, we study the estimation problem of state and activation signals. Due to the relation (7), it is sufficient to estimate the state and unknown inputs of the system (19)–(25).

III. OBSERVER DESIGN

In this section, we introduce three methods to estimate the state variables and the activation signals: a high gain observer, a sliding mode observer, and an adaptive sliding observer. The convergence analysis of the three observers is provided. A discussion of the comparison of the three observers is presented.

Denote the estimates of x, u, and $a = [a_1, a_2]^T$ as

$$\hat{x} = \begin{bmatrix} \hat{x}_1 & \hat{x}_2 & \hat{x}_3 & \hat{x}_4 \end{bmatrix}^T \quad (27)$$

$$\hat{u} = \begin{bmatrix} \hat{u}_1 & \hat{u}_2 \end{bmatrix}^T \quad (28)$$

$$\hat{a} = \begin{bmatrix} \hat{a}_1 & \hat{a}_2 \end{bmatrix}^T. \quad (29)$$

3.1 High gain observer

The high gain observer in this subsection is designed based on the extended high gain observer approach reported in [10,11]. The structure of the proposed high gain observer is described as

$$\dot{\hat{x}}_1 = \hat{x}_2 + \frac{h_{11}}{\epsilon_h}(y_1 - \hat{x}_1) \tag{30}$$

$$\dot{\hat{x}}_2 = \frac{1}{m}(y_3 - y_2) + \hat{\Delta}_\Phi(t) \quad + \frac{h_{12}}{\epsilon_h^2}(y_1 - \hat{x}_1) \tag{31}$$

$$\dot{\hat{\Delta}}_\Phi = \frac{h_{13}}{\epsilon_h^3}(y_1 - \hat{x}_1) \tag{32}$$

$$\dot{\hat{x}}_3 = \hat{x}_2 + \hat{u}_1 + \frac{h_{21}}{\epsilon_h}(\Phi_{S1}^{-1}(y_2) - \hat{x}_3) \tag{33}$$

$$\dot{\hat{u}}_1 = \frac{h_{22}}{\epsilon_h^2}(\Phi_{S1}^{-1}(y_2) - \hat{x}_3) \tag{34}$$

$$\dot{\hat{x}}_4 = -\hat{x}_2 + \hat{u}_2 + \frac{h_{31}}{\epsilon_h}(\Phi_{S2}^{-1}(y_3) - \hat{x}_4) \tag{35}$$

$$\dot{\hat{u}}_2 = \frac{h_{32}}{\epsilon_h^2}(\Phi_{S2}^{-1}(y_3) - \hat{x}_4), \tag{36}$$

where $\epsilon_h \in (0,1)$ is a design parameter, parameters h_{11}, h_{12}, h_{13} are chosen such that the polynomial $s^3 + h_{11}s^2 + h_{12}s + h_{13}$ is Hurwitz, parameters h_{ij} for $i = 2,3$ and $j = 1,2$ are chosen such that the polynomials $s^2 + h_{i1}s + h_{i2}$ are Hurwitz for $i = 2,3$ [10].

Theorem 1. Under Assumptions 1 and 2, the state and input estimates of the high gain observer presented in (30)–(36) satisfy $\|x(\tau) - \hat{x}(\tau)\| \to 0$ and $\|u_j(\tau) - \hat{u}_j(\tau)\| \to 0$ for $j = 1,2$ as $\epsilon_h \to 0$ for $\tau \geq 0$.

Proof. The proof is based on the construction of the extended high gain observer in [10,11].

Remark 2. Theorem 1 states that if $\epsilon_h \to 0$, the state and unknown input estimates will be exactly the true values. Since $\epsilon_h \neq 0$, a practical choice of ϵ_h lies in $(0,1)$.

Remark 3. The high gain observer requires the tuning of nine parameters: ϵ_h, h_{11}, h_{12}, h_{13}, h_{21}, h_{22}, h_{31}, h_{32}.

3.2 Sliding mode observer

Following the super twisting algorithm and the traditional sliding mode approach in [9,15], the sliding mode observer for our system possesses the following structure:

$$\dot{\hat{x}}_1 = \hat{x}_2 + v_{11} \tag{37}$$

$$\dot{\hat{x}}_2 = \frac{1}{m}(y_3 - y_2) + v_{12} \tag{38}$$

$$\dot{\hat{x}}_3 = \hat{x}_2 + v_2 \tag{39}$$

$$\dot{\hat{x}}_4 = -\hat{x}_2 + v_3 \tag{40}$$

where

$$v_{11} = \lambda_{11}\,|y_1 - \hat{x}_1|^{1/2}\text{sign}(y_1 - \hat{x}_1) \tag{41}$$

$$v_{12} = \alpha_{11}\,\text{sign}(y_1 - \hat{x}_1) \tag{42}$$

$$v_2 = \alpha_2\,\text{sign}(\Phi_{S1}^{-1}(y_2) - \hat{x}_3) \tag{43}$$

$$v_3 = \alpha_3\,\text{sign}(\Phi_{S2}^{-1}(y_3) - \hat{x}_4). \tag{44}$$

Here λ_{11} and α_{11} are design parameters which can be chosen to satisfy the following inequalities [9]:

$$\alpha_{11} > f^+ \tag{45}$$

$$\lambda_{11} > \sqrt{\frac{2}{\alpha_{11} - f^+}}\,\frac{(\alpha_{11} + f^+)(1+p)}{(1-p)} \tag{46}$$

where p is a positive constant such that $0 < p < 1$, $f^+ > 0$ is the upper bound of Δ_Φ: $|\Delta_\Phi| < f^+$. The parameters α_2 and α_3 in (43) and (44) are chosen such that [15]

$$U_{1m} < \alpha_2 \tag{47}$$

$$U_{2m} < \alpha_3 \tag{48}$$

where U_{1m} and U_{2m} are defined in (13). The reconstruction of the uncertainty Δ_Φ and unknown inputs u_1 and u_2 is accomplished with low pass filters given as

$$\tau_s\,\dot{\hat{\Delta}}_\Phi = -\hat{\Delta}_\Phi + v_{12} \tag{49}$$

$$\tau_s\,\dot{\hat{u}}_1 = -\hat{u}_1 + v_2 \tag{50}$$

$$\tau_s\,\dot{\hat{u}}_2 = -\hat{u}_2 + v_3 \tag{51}$$

where τ_s is a positive parameter.

Theorem 2. Under Assumptions 1 and 2, there exists a positive number $\tau^\star$ such that the state and input estimates of the high gain observer presented in (37)–(40) and (49)–(51) satisfy $x(\tau) - \hat{x}(\tau) = 0$ and $u(\tau) \to \hat{u}(\tau)$ for $\tau \geq \tau^\star$.

Proof. The proof follows the super-twisting algorithm and the standard sliding mode in [9,15]. Let

$$e = x - \hat{x}. \tag{52}$$

The state estimation dynamics are

$$\dot{e}_1 = e_2 - v_{11} \tag{53}$$

$$\dot{e}_2 = \Delta_\Phi(\tau) - v_{12} \tag{54}$$

$$\dot{e}_3 = e_2 + u_1 + v_2 \tag{55}$$

$$\dot{e}_4 = -e_2 + u_2 + v_3. \tag{56}$$

According to [9], there exists a number $\tau_1^\star > 0$ such that $e_1(\tau) = 0$ and $e_2(\tau) = 0$ for $\tau \geq \tau_1^\star$. It is easy to show that e_3 and e_4 are bounded in the interval $[0, \tau_1^\star]$. Since the error dynamics of e_3 is the first order sliding mode for $\tau \geq \tau_1^\star$, there exists a number $\tau_2^\star \geq \tau_1^\star$ such that $e_3(\tau) = 0$ for $\tau \geq \tau_2^\star$ [15]. Using the same argument, there exists a number $\tau_3^\star \geq \tau_1^\star$ such that $e_4(\tau) = 0$ for $\tau \geq \tau_3^\star$. Therefore, $e = 0$ for $\tau \geq \tau^\star = \max\{\tau_1^\star, \tau_2^\star, \tau_3^\star\}$.

According to [9,15], the injection signals v_{12}, v_2, and v_3 are employed to estimate Δ_Φ, u_1, and u_2 in (49), (50), (51), from which $\hat{\Delta}_\Phi \to \Delta_\Phi$ and $\hat{u} \to u$.

Remark 4. A practical implementation of the sign function of the sliding mode observer is $\text{sign}(e) \approx \frac{e}{\delta_s + |e|}$, which adds another design parameter, namely δ_s.

Remark 5. The proposed sliding mode observer requires the tuning of six parameters: λ_{11}, α_{11}, α_2, α_3, τ_s, δ_s.

Remark 6. The parameters of the sliding mode observer depend explicitly on the information of the bounds of the unknown inputs and uncertainty.

3.3 Adaptive sliding mode observer

The adaptive sliding mode observer for our system is designed based on the dual layer nested adaptive approaches in [13,14]. The proposed adaptive sliding mode observer is given as follows:

$$\begin{aligned}\dot{\hat{x}}_1 &= \hat{x}_2 + \alpha_a(\tau)\,|y_1 - \hat{x}_1|^{1/2}\text{sign}(y_1 - \hat{x}_1) \\ &\quad - \phi(y_1 - \hat{x}_1, L_a)\end{aligned} \tag{57}$$

$$\dot{\hat{x}}_2 = \beta_a(\tau)\text{sign}(y_1 - \hat{x}_1) \tag{58}$$

$$\dot{\hat{\Delta}}_\Phi = \frac{1}{\tau_a}(-\hat{\Delta}_\Phi - \beta_a(\tau)\text{sign}(y_1 - \hat{x}_1) \tag{59}$$

$$\dot{\hat{x}}_3 = (k_1(\tau) + \eta_1)\text{sign}(\Phi_{S1}^{-1}(y_2) - \hat{x}_3) \tag{60}$$

$$\dot{\hat{u}}_1 = \frac{1}{\tau_a}(-\hat{u}_1 - (k_1(\tau) + \eta_1)\text{sign}(\Phi_{S1}^{-1}(y_2) - \hat{x}_3)) \tag{61}$$

$$\dot{\hat{x}}_4 = (k_2(\tau) + \eta_2)\text{sign}(\Phi_{S2}^{-1}(y_3) - \hat{x}_4) \tag{62}$$

$$\dot{\hat{u}}_2 = \frac{1}{\tau_a}(-\hat{u}_2 - (k_2(\tau) + \eta_2)\text{sign}(\Phi_{S2}^{-1}(y_3) - \hat{x}_4)) \tag{63}$$

where τ_a, η_1, and η_2 are positive design parameters,

$$\alpha_a(\tau) = \sqrt{L_a(\tau)}\,\alpha_0 \tag{64}$$

$$\beta_a(\tau) = L_a(\tau)\,\beta_0, \tag{65}$$

where α_0 and β_0 are fixed positive scalars and

$$\phi(e_1, L_a) = -\frac{\dot{L}_a(\tau)}{L_a(\tau)}\,e_1(\tau). \tag{66}$$

Define

$$\delta_{a0}(\tau) = L_a(\tau) - \frac{1}{a\beta_0}\,|\hat{\Delta}_\Phi| - \epsilon_a \tag{67}$$

where a is chosen such that $0 < a < 1/\beta_0 < 1$ and ϵ_a is a small positive scalar chosen to satisfy

$$\frac{1}{a\beta_0}\,|\hat{\Delta}_\Phi| + \epsilon_a/2 > |\Delta_\Phi|. \tag{68}$$

The proposed adaptive element $L_a(\tau)$ is given by

$$L_a(\tau) = l_0 + l_a(\tau) \tag{69}$$

where l_0 is a small positive design constant and

$$\dot{l}_a(\tau) = -\rho_{a0}(\tau)\text{sign}(\delta_a(\tau)). \tag{70}$$

The time-varying term in (70) is given by

$$\rho_{a0}(\tau) = r_{00} + r_{a0}(\tau) \tag{71}$$

where r_{00} is a positive design parameter,

$$\dot{r}_{a0}(\tau) = \begin{cases} \gamma_{a0}\,|\delta_{a0}(\tau)| & \text{if } |\delta_{a0}(\tau)| > \delta_{00} \\ 0 & \text{otherwise} \end{cases} \tag{72}$$

where δ_{a0} is defined in (67), $\gamma_{a0} > 0$ and $\delta_{00} > 0$ are design parameters. For $j = 1, 2$, define

$$\delta_{aj}(\tau) = k_j(\tau) - \frac{1}{\alpha_{aj}}\,|\hat{u}_j| - \epsilon_{aj} \tag{73}$$

where α_{aj} is chosen such that $0 < \alpha_{aj} < 1$ and $\epsilon_{aj} > 0$ is a small positive scalar chosen to satisfy

$$\frac{1}{\alpha_{aj}}\,|\hat{u}_j| + \epsilon_{aj}/2 > |u_j|. \tag{74}$$

The proposed adaptive elements $k_j(\tau)$ are given by

$$\dot{k}_j(\tau) = -\rho_{aj}(\tau)\text{sign}(\delta_{aj}(\tau)) \tag{75}$$

for $j = 1, 2$. The time-varying terms in (75) are given by

$$\rho_{aj}(\tau) = r_{0j} + r_{aj}(\tau), \text{ for } j = 1, 2 \tag{76}$$

where r_{0j} is a positive design parameter and

$$\dot{r}_{aj}(\tau) = \begin{cases} \gamma_{aj}\,|\delta_{aj}(\tau)| & \text{if } |\delta_{aj}(\tau)| > \delta_{0j} \\ 0 & \text{otherwise} \end{cases} \tag{77}$$

where $\gamma_{aj} > 0$ and δ_{0j} is a small positive parameter.

Theorem 3. Under Assumptions 1 and 2, there exists a positive number $\tau^\dagger$ such that the state and input estimates of the high gain observer presented in (57)–(63) satisfy $x(\tau) - \hat{x}(\tau) = 0$ and $u(\tau) \to \hat{u}(\tau)$ for $\tau \geq \tau^\dagger$.

Proof. The proof follows the results of the dual layer nested adaptive approaches in [13,14]. The error dynamics for the state estimation are

$$\dot{e}_1 = e_2 - \alpha_a(\tau)\,|e_1|^{1/2}\text{sign}(e_1) - \phi(e_1, L_a) \tag{78}$$

$$\dot{e}_2 = \Delta_\Phi - \beta_a(\tau)\text{sign}(e_1) \tag{79}$$

$$\dot{e}_3 = e_2 - (k_1(\tau) + \eta_1)\text{sign}(e_3) \tag{80}$$

$$\dot{e}_4 = -e_2 - (k_2(\tau) + \eta_2)\text{sign}(e_4). \tag{81}$$

According to [14], there exists a number $\tau_1^\dagger > 0$ such that $e_1(\tau) = 0$ and $e_2(\tau) = 0$ for $\tau \geq \tau_1^\dagger$. It is easy to show that e_3 and e_4 are bounded in the interval $[0, \tau_1^\dagger]$.

According to [13], there exists a number $\tau_2^\dagger \geq \tau_1^\dagger$ such that $e_3(\tau) = 0$ for $\tau \geq \tau_2^\dagger$ [15]. Using the same argument, there exists a number $\tau_3^\dagger \geq \tau_1^\dagger$ such that $e_4(\tau) = 0$ for $\tau \geq \tau_3^\dagger$. Therefore, $e = 0$ for $\tau \geq \tau^\dagger = \max\{\tau_1^\dagger, \tau_2^\dagger, \tau_3^\dagger\}$.

The recovery of Δ_Φ, u_1, and u_2 follows the standard filtering approach in sliding mode control [15] in (59), (61), (63), from which $\hat{\Delta}_\Phi \to \Delta_\Phi$ and $\hat{u} \to u$.

Remark 7. Similar to the traditional sliding mode observer, the sign function of the adaptive sliding mode observer can be approximated as $\text{sign}(e) \approx \frac{e}{\delta_a + |e|}$, which introduces another design parameter, that is δ_a.

Remark 8. The proposed adaptive sliding mode observer requires the tuning of 21 parameters: α_0, β_0, η_1, η_2, a, l_0, $r_{00}, r_{01}, r_{02}, \tau_a, \epsilon_{a1}, \epsilon_{a2}, \alpha_{a1}, \alpha_{a2}, \gamma_{a0}, \gamma_{a1}, \gamma_{a2}, \delta_{00}, \delta_{01}, \delta_{02}, \delta_a$. The tuning of the parameters was presented above. For more details, see [13,14].

Remark 9. The parameters of the adaptive sliding mode observer in general do not depend on the bounds of the unknown inputs and uncertainty.

3.4 Discussion

As presented above, the high-gain observer requires the tuning of nine parametes, the traditional sliding mode observer needs six parameters, and the adaptive high gain observer uses 21 parameters. All of the observers can estimate state variables and unknown inputs in the presence of uncertainties. The traditional sliding mode observer requires the least number of parameters but partial knowledge of bounds of uncertainties and unknown inputs is required. Meanwhile, the adaptive sliding mode observer has an advantage over the traditional sliding mode observer in the sense that it does not need any knowledge of unknown inputs and uncertainties but its structure is the most complicated. The high-gain observer is flexible in terms of the number of parameters but the tuning of parameters depends on the experience or trial-and-error tests of the designer. In addition, the high-gain observer can produce high peaks during transients due to its high gain.

IV. NUMERICAL EXAMPLE

For the purpose of estimation, we employ a backstepping controller for the output L_{m1} to track a time-varying reference signal. A numerical example will be conducted using the proposed controller and observers to estimate the state variables and the activation signals.

4.1 Backstepping controller

In this paper, a tracking control scheme is constructed based on its counterpart for setpoint regulation [16].

Denote the reference signal as $r(t)$ and assume that it is twice differentiable.

Denote the tracking error and its derivative as

$$e = \begin{bmatrix} e_1 \\ e_2 \end{bmatrix} = \begin{bmatrix} x_1 - r \\ \dot{x}_1 - \dot{r} \end{bmatrix}. \tag{82}$$

Furthermore, define

$$\zeta = \Phi_{S2}(L_{S2}) - \Phi_{S1}(L_{S1}) + m\Delta_\Phi - m\dot{r}. \tag{83}$$

Our goal is to design u_1 and u_2 such that e converges to 0. The error dynamics is described in the form

$$\dot{e} = Ae + B\zeta \tag{84}$$

where

$$A = \begin{bmatrix} 0 & 1 \\ 0 & 0 \end{bmatrix}, \quad B = \begin{bmatrix} 0 \\ \frac{1}{m} \end{bmatrix}. \tag{85}$$

Consider the Lyapunov function

$$V = \frac{1}{2}e^T P e \tag{86}$$

where P is a positive definite matrix. The system (84) is stable if a state feedback regulator is chosen as

$$\zeta = \Psi(e) = -Ke \tag{87}$$

such that $A_{cl} = A - BK$ is Hurwitz. Hence,

$$\dot{V} = \frac{1}{2}e^T(A_{cl}^T P + PA_{cl})e = -\frac{1}{2}e^T Q e \tag{88}$$

where Q is positive definite. Thus, $\dot{V} < 0$. This implies that the error converges to 0. However, ζ is

not a direct control input. As a result, we introduce a variable

$$w = \zeta - \Psi(e). \tag{89}$$

Its derivative is given as $\dot{w} = \dot{\zeta} - \dot{\Psi}(e) = \Phi'_{S2}\dot{L}_{S2} - \Phi'_{S1}\dot{L}_{S1} + m\dot{\Delta}_\Phi - m\ddot{r}$ where $\Phi'_{Si} = \frac{d\Phi_{Si}}{dL_{Si}}$ for $i = 1, 2$.

The error dynamics is rewritten as

$$\dot{e} = A_{cl}e + Bw \tag{90}$$

Augment the Lyapunov function V with a quadratic term

$$V_a = V + \frac{1}{2}w^2. \tag{91}$$

Taking its derivative yields $\dot{V}_a = -\frac{1}{2}e^T Qe + w\kappa$ where $\kappa = \Phi'_{S2}(x_2 + u_2) - \Phi'_{S1}(-x_2 + u_1) + dm\dot{\Delta}_\Phi - m\ddot{r} + B^T Pe$.

Here, κ is chosen such that

$$\kappa = -\gamma w \tag{92}$$

with $\gamma > 0$ to make $\dot{V}_a$ negative definite. Hence, the augmented system of e and w is asymptotically stable. It should be noted that we cannot deduce unique solutions of u_1 and u_2 from κ in (92).

From (92), $\Phi'_{S2}u_2 - \Phi'_{S1}u_1 = \beta$ where $\beta = -K_1\zeta - K_2 e - (\Phi'_{S2} + \Phi'_{S1})x_2 + m\ddot{r}$ with $K_1 = \gamma + KB$, and $K_2 = (KA + \gamma K + B^T P)e$.

Similar to [16], the least square virtual control inputs are given as $u_1 = -\frac{\Phi'_{S1}}{\Delta}\beta$ and $u_2 = \frac{\Phi'_{S2}}{\Delta}\beta$ where $\Delta = (\Phi'_{S1})^2 + (\Phi'_{S2})^2$.

Table I. Controller parameters.

Parameter	Equation	Value
K	equation (87)	$\begin{bmatrix} 0.5774 & 1.2198 \end{bmatrix}$
Q	equation (88)	$\begin{bmatrix} 10 & 0 \\ 0 & 10 \end{bmatrix}$
P	equation (88)	$\begin{bmatrix} 21.1284 & 17.3205 \\ 17.3205 & 36.5955 \end{bmatrix}$
γ	equation (92)	1

Table II. HGO parameters.

Parameter	Equation	Value
ϵ_h	equations (30)-(36)	0.1
h_{11}	equation (30)	3
h_{12}	equation (31)	3
h_{13}	equation (32)	1
h_{21}	equation (33)	2
h_{22}	equation (34)	1
h_{31}	equation (35)	2
h_{32}	equation (36)	1

4.2 Simulation

To illustrate the proposed schemes, we conducted a numerical simulation for a dual muscle system. The total length of the dual muscle system is $C = Lm_1 + Lm_2 = 5.54$. The mass of the system is $m = 1$. The reference trajectory is chosen as $r = 2.6315 + 0.01 \sin 0.5\tau$.

Functions Φ_{Sj}, Φ_{Pj} are chosen as in (17) and (18), [17]. The parameter of (8) is $W = 0.3$. The parameters of (9) are chosen as: $A = 0.25$, $g_{max} = 1.5$.

The upper bound of $\Phi_{S2}(x_4) - \Phi_{S1}(x_3)$ is 1. The uncertainty of the system is $\Delta_\Phi(\tau) = 0.005 + 0.005 \sin 0.8\tau$.

The controller parameters in Subsection 4.1 are presented in Table I. The parameters for the high gain observer (HGO) are presented in Table II. The tuning of the parameters was shown in Section 3.1. The parameters for the sliding mode observer (SMO) are presented in Table III. The tuning of the parameters was shown in Section 3.2. The parameters for the adaptive sliding mode observer (ASMO) are presented in Table IV. The parameters are chosen according to [23, 24].

Table III. SMO parameters.

Parameter	Equation	Value
α_{11}	equation (45)	1.1
λ_{11}	equation (46)	28.17
α_2	equation (47)	1.1
α_3	equation (48)	1
τ_s	equations (49)–(51)	0.01
δ_s	equation in Remark 4	0.01

Table IV. ASMO parameters.

Parameter	Equation	Value
α_0	equation (64)	1.1
β_0	equation (65)	2.97
η_1	equations (60), (61)	0.2
η_2	equations (62), (63)	0.2
a	equation (67)	0.82
l_0	equation (69)	0.4
r_{00}	equation (71)	0.4
r_{01}, r_{02}	equation (76)	0.5
τ_a	equations (59), (61), (63)	0.01
ϵ_{a1}	equation (73)	0.2
ϵ_{a2}	equation (73)	0.2
α_{a1}, α_{a2}	equation (73)	0.99
γ_{a0}	equation (72)	200
γ_{a1}, γ_{a2}	equation (77)	300
δ_{00}	equation (72)	0.001
δ_{01}, δ_{02}	equation (77)	0.001
δ_a	equation in Remark 7	0.01

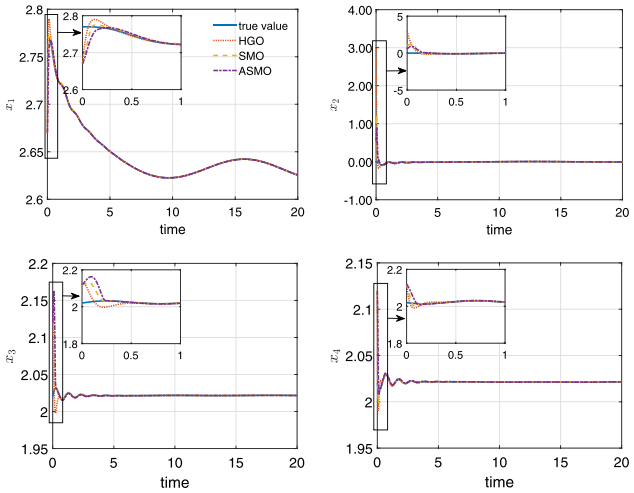

Fig. 2. The true value and estimates of x using 3 observers: high gain observer (HGO), sliding mode observer (SMO), adaptive sliding mode observer (ASMO). [Color figure can be viewed at wileyonlinelibrary.com]

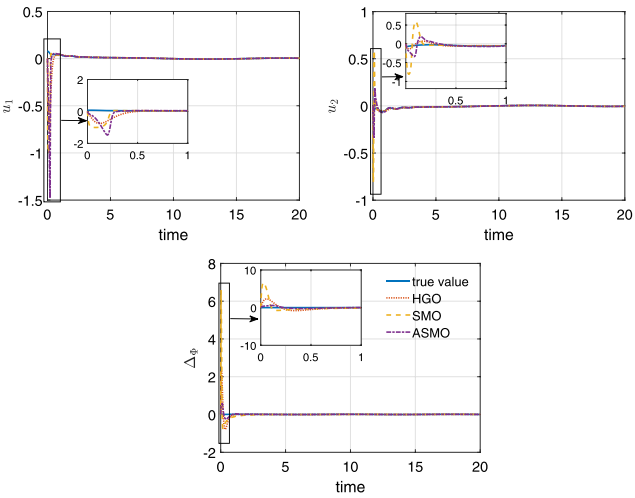

Fig. 3. The true value and estimates of u and Δ_Φ using 3 observers: high gain observer (HGO), sliding mode observer (SMO), adaptive sliding mode observer (ASMO). [Color figure can be viewed at wileyonlinelibrary.com]

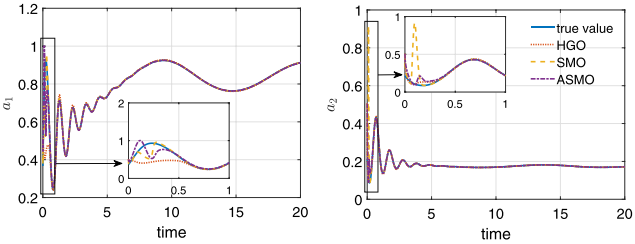

Fig. 4. The true value and estimates of a using 3 observers: high gain observer (HGO), sliding mode observer (SMO), adaptive sliding mode observer (ASMO). [Color figure can be viewed at wileyonlinelibrary.com]

Note that the model under consideration is dimensionless as pointed out in Section II. Hence, there are no units specified on axes in the following figures.

4.3 Results discussion

It is shown in Fig. 2 that the estimates of x_1, x_2, x_3, x_4 using the three observers converge to their true values at about $\tau = 0.5$. It is seen that the estimates using the HGO exhibit peaks during transients while the SMO and ASMO do not possess such problems. Fig. 3 depicts the evolution of the estimates of the uncertainty Δ_Φ and unknown inputs u_1 and u_2, which track well their true values. The estimates of the activation signals shown in Fig. 4 converge to their true values. The closeness of the estimates and their true values reveals that the estimation schemes are effective in estimating the state variables and activation signals.

The simulation illustrates that the three observers are comparably effective in estimating the state variables and activation signals of the dual muscle system. Note that the three observers have a lot of freedom in tuning parameters. While the ASMO does not require knowledge of the bounds of the unknown inputs and uncertainty, the SMO offers more simple tuning with fewer parameters. Although the HGO provides good estimates, it can produce high peaks during transients, which in some cases are not desired.

V. CONCLUSIONS

In this paper, we have presented the agonistic-antagonistic muscle system based on the Hill muscle model. Three estimation approaches have been introduced to estimate the state variables and activation signals. A numerical simulation was conducted to demonstrate the efficiency of the proposed schemes.

The dual muscle system considered in this paper serves as a basic element in complicated muscle systems with multi-muscle multi-joint structures. In future work, the estimation problems of these systems will face interconnection structures and output measurement with nonlinear components. In addition, experimental tests will be carried out to validate the proposed estimation schemes. Possible challenges include calibration and scaling of system structures in experiments.

REFERENCES

1. Zajac, F. E., "Muscle and tendon: Properties, models, scaling, and application to biomechanics and motor," *Critical Reviews in Biomedical Engineering*, Vol. 17, No. 4, pp. 359–411 (1989).
2. Winters, J. M., "Hill–based muscle models: A systems engineering perspective." *Multiple Muscle Systems: Biomechanics and Movement Organization*, Ch. 5, Springer, New York (1990).
3. Buchanan, T. S., D. G. Lloyd, K. Manal, and T. F. Besier, "Neuromusculoskeletal modeling: Estimation of muscle forces and joint moments and movements from measurements of neural command," *J. Appl. Biomech.*, Vol. 20, No. 4, pp. 367 (2004).
4. Erdemir, A., S. McLean, W. Herzog, and A. J. van den Bogert, "Model-based estimation of muscle forces exerted during movements," *Clin. Biomech.*, Vol. 22, No. 2, pp. 131–154 (2007).
5. Mohammed, S., W. Huo, J. Huang, H. Rifaï, and Y. Amirat, "Nonlinear disturbance observer based sliding mode control of a human-driven knee joint orthosis," *Robot. Auton. Syst.*, Vol. 75, No. PA, pp. 41–49 (2016).
6. Yamasaki, T., K. Idehara, and X. Xin, "Estimation of muscle activity using higher-order derivatives, static optimization, and forward-inverse dynamics," *J. Biomech.*, Vol. 49, No. 10, pp. 2015–2022 (2016).
7. Lin, Y.-C., J. P. Walter, S. A. Banks, M. G. Pandy, and B. J. Fregly, "Simultaneous prediction of muscle and contact forces in the knee during gait," *J. Biomech.*, Vol. 43, No. 5, pp. 945–952 (2010).
8. Edwards, C., S. K. Spurgeon, and R. J. Patton, "Sliding mode observers for fault detection and isolation," *Automatica*, Vol. 36, No. 4, pp. 541–553 (2000).
9. Davila, J., L. Fridman, and A. Levant, "Second-order sliding-mode observer for mechanical systems," *IEEE Trans. Automatic Control*, Vol. 50, No. 11, pp. 1785–1789 (2005).
10. Lee, J., R. Mukherjee, and H. K. Khalil, "Output feedback stabilization of inverted pendulum on a cart in the presence of uncertainties," *Automatica*, Vol. 54, pp. 146–157 (2015).
11. Lee, J., R. Mukherjee, and H. K. Khalil, "Output feedback performance recovery in the presence of uncertainties," *Syst. Control Lett.*, Vol. 90, pp. 31–37 (2016).
12. Nguyen, T., S. G. Khan, T. Hatano, et al., "Real-time sliding mode observer scheme for shear force estimation in a transverse dynamic force microscope," *Asian J. Control*, Vol. 20, No. 4, pp. 1317–1328 (2018).
13. Edwards, C. and Y. B. Shtessel, "Adaptive continuous higher order sliding mode control," *Automatica*, Vol. 65, pp. 183–190 (2016).
14. Edwards, C. and Y. Shtessel, "Adaptive dual-layer super-twisting control and observation," *Int. J. Control*, Vol. 89, No. 9, pp. 1759–1766 (2016).
15. Edwards, C. and S. Spurgeon, *Sliding Mode Control: Theory and Applications*, CRC Press, London (1998).

16. Richter, H. and H. Warner, "Stable Nonlinear Control of an Agonist-Antagonist Muscle-Driven System," *IFAC-PapersOnLine*, Vol. 50, No. 1, pp. 7199–7204 (2017).
17. Warner, H. and H. Richter. Non-dimensional modeling and simulation of an agonist-antagonist muscle-driven system. *Technical Report Tech. Rep.*, Cleveland State University, Department of Mechanical Engineering, Oct 2016. available at http://academic.csuohio.edu/richter_h/lab/simulationReport.pdf.
18. Hermann, R. and A. Krener, "Nonlinear controllability and observability," *IEEE Trans. Autom. Control*, Vol. 22, No. 5, pp. 728–740 (1977).
19. Xiao, B. and S. Yin, "Exponential tracking control of robotic manipulators with uncertain kinematics and dynamics," *IEEE Trans. Ind. Inform.* Available at: https://ieeexplore.ieee.org/document/8302510/.
20. Wang, Y., H. Shen, H. R. Karimi, and D. Duan, "Dissipativity-based fuzzy integral sliding mode control of continuous-time T-S fuzzy systems," *IEEE Trans. Fuzzy Syst.*, Vol. 26, No. 3, pp. 1164–1176 (2018).
21. Galván-Guerra, R., L. Fridman, R. Iriarte, and M. Steinberger, "Integral sliding-mode observation and control for switched uncertain linear time invariant systems: A Robustifying strategy," *Asian J. Control*, Vol. 20, No. 6, pp. 1–15 (2018).
22. Lau, J. Y., W. Liang, H. C. Liaw, and K. K. Tan, "Sliding mode disturbance observer-based motion control for a piezoelectric actuator-based surgical device," *Asian J. Control*, Vol. 20, No. 3, pp. 1194–1203 (2018).

Thang Tien Nguyen is affiliated with Modeling Evolutionary Algorithms Simulation and Artificial Intelligence, Faculty of Electrical & Electronics Engineering, Ton Duc Thang University, Ho Chi Minh City, Vietnam. He received his B.Eng. and M.S. degrees from Hanoi University of Technology, Hanoi, Vietnam, in 2002 and 2004 respectively, and his Ph.D. degree from Rutgers University, NJ, USA, in 2010. His research interests include optimization, optimal control, adaptive control, sliding mode control, Atomic Force Microscope, and robotics.

Holly Warner received a BS degree and an MS degree in mechanical engineering from Cleveland State University, Cleveland, OH, USA in 2014 and 2015, respectively. She is now performing research as a doctoral student within the Department of Mechanical Engineering at Cleveland State University, Cleveland, OH, USA. Her research interests include modeling, control, and optimization of human and robotic systems with an emphasis in the area of prosthetic devices.

Hung La is the Director of the Advanced Robotics and Automation (ARA) Lab, and Assistant Professor of the Department of Computer Science and Engineering, University of Nevada, Reno, NV, USA. His research interests include robotics, mobile sensor networks, cooperative control, learning and sensing, systems and controls, automation science and engineering.

Hanieh Mohammadi received the B.S. and M.S. degrees in electrical engineering from Shiraz University, Shiraz, Iran, in 2011 and 2013, respectively. She is currently a Doctoral researcher in the Department of Electrical Engineering and Computer Science, Cleveland State University, Cleveland, OH, USA. Her research interests include exercise machine, prosthetics, Kalman filter, state estimation, machine learning, and evolutionary optimization.

Dan Simon is the Associate Vice President for Research, and Professor of Electrical Engineering and Computer Science at Cleveland State University (CSU), Cleveland, OH, USA. He has conducted research on many technologies, including prosthetics, robotics, aircraft engines, motor control, electrocardiogram signal processing, environmental monitoring, satellite design, and others. He has written three books and has published almost 200 refereed journal and conference publications, which have been cited over 10,000 times. As principal investigator he has been awarded over 2.5 million in research funding from the NSF, NASA, Cleveland Clinic, and industry.

Hanz Richter is currently a Professor in the Mechanical Engineering Department, Cleveland State University, Cleveland, OH, USA. His projects are in the fields of biomedical robots and prostheses, advanced exercise machine, aeroengine propulsion control, and high-precision motion control, among others. His research interests include control theory and applications, robotics, and mechatronics.